# Infrared and Submillimeter Observations of CB130

**Hyo Jeong Kim (U. Texas; *hyojeong@astro.as.utexas.edu*), The c2d Team (Multiple Institutions)**


## Abstract

**We present a study of three small dark clouds in CB130. The *Spitzer Space Telescope* discovered two young stellar objects in the CB130-1 core. The *Spitzer* and ground-based telescopes have observed CB130-1 in the infrared and the submillimeter regions. The photometry data from 3.6 μm to 850 μm give us constraints on the radiative transfer modeling. Through the modeling we can figure out the internal luminosity of the young stellar object in CB130-1 core. The more embedded of the two young stellar objects has an internal luminosity, 0.15 $L_\odot$, which is a low value for a young star. We also present the molecular line observation data of the three cores in CB130. Also, we calculate gas temperature of CB130-1 and use an ad hoc step function abundance for Monte Carlo simulation inputs. The step function abundance model fits observed lines reasonably well.**


## Introduction

- The *Spitzer* Legacy Project, C2D "From Molecular Cores to Planet forming Disks", completes database of nearby low mass star forming regions. The *Spitzer space telescope* has identified about 12 low luminosity protostars within cores previously considered to be starless (for example, L1014(Young et al., 2004), IRAM04191+1522(Dunham et al., 2006), and L1521F(Bourke et al., 2006)).
- The standard model (Shu, 1987) accretion luminosity : $L_{acc} \sim 1.6L_\odot$
  L1014, IRAM04191+1522, L1521F are Very Low Luminosity Objects (VeLLOs : $L_{int} \leq 0.1L_\odot$ (Di Francesco et al, 2006) ).
- Low luminosity young stellar objects can be a good laboratory to understand low mass star or brown dwarf formation.
  The Episodic Accretion Model may explain the low accretion luminosity of these objects.

## CB130

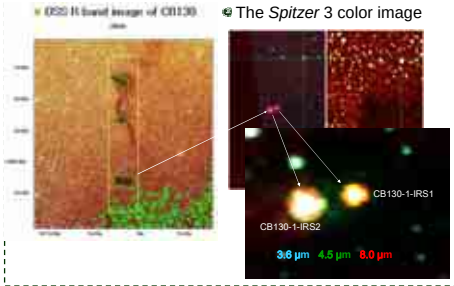


- The *Spitzer* 3 color image

- The Spitzer observation detected two young stellar objects in the CB130-1 region.
- CB130 is located at the Aquila Rift region.
- First appears at the catalog of Clemens & Barvainis (1988).
- Lee & Myers (1999) located three separate dense regions in CB130

- RA 18h 16m 16s
- DEC -02°16' ~ 33'
- Distance 270pc

## Observation & Result

### Color-Color Diagram

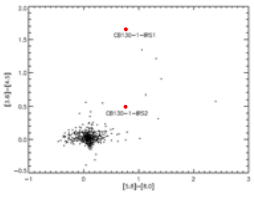

Compared to the background stars CB130-1-IRS1 and CB130-1-IRS2 are red.

### SED of CB130-1-IRS1

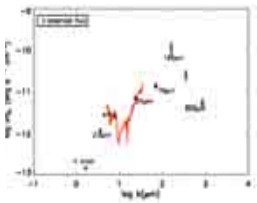

- $L_{bol} = 0.23L_\odot$
- $T_{bol} = 59 \pm 1.6K$
- $L_{bol}/L$ (>350μm) ~ 9.1

⇒ **Class 0 object**

### SED of CB130-1-IRS2

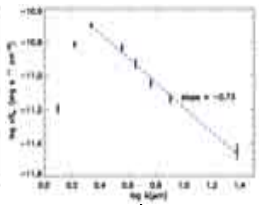

- Spectral index at **λ**>2.2 **μ**m : -0.73.
- IRS2 was not detected at **λ**>70 **μ**m
- $L_{bol} = 0.076\ L_\odot$
- $T_{bol} = 1150 \pm 14K$

⇒ **Class II object**

### FCRAO Molecular Line Map

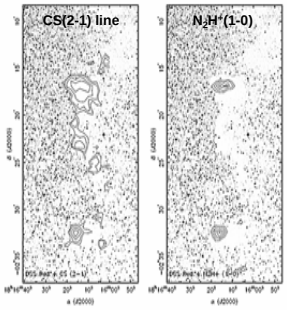


- CS (2-1) is detected at all three cores.
- $N_2H^+$ (1-0) is detected at CB130-1 and CB130-3 only.

### The summary of molecular line observations

CB130-1

| | $\int T_A^* dv$(K km s$^{-1}$) | $v_{LSR}$(km s$^{-1}$) | $\Delta v$(km s$^{-1}$) | $T_A^*$(K) | Telescope |
|---|---|---|---|---|---|
| CO 2-1 | 9.38 | 8.27 | 4.73 | 1.86 | CSO |
| $C^{18}O$ 2-1 | 0.48 | 7.61 | 0.71 | 0.64 | CSO |
| $H^{13}CO^+$ 3-2 | 0.070 | 7.88 | 0.28 | 0.24 | CSO |
| $HCO^+$ 3-2 | 0.82 | 7.67 | 0.60 | 1.3 | CSO |
| $N_2H^+$ 3-2 | 0.45 | 7.62 | 0.88 | 0.49 | CSO |
| $N_2H^+$ 1-0 | 2.27 | 7.35 | 1.07 | 0.99 | ARO |
| $N_2H^+$ 1-0 | 1.30 | 7.43 | 0.44 | 0.38 | FCRAO |
| CS 2-1 | 0.29 | 7.78 | 0.54 | 0.43 | FCRAO |
| $N_2D^+$ 3-2 | ... | ... | ... | < 0.23 | CSO |
| $N_2D^+$ 1,1,0 - 1,1,1 | ... | ... | ... | < 0.29 | CSO |

CB130-2

| | $\int T_A^* dv$(K km s$^{-1}$) | $v_{LSR}$(km s$^{-1}$) | $\Delta v$(km s$^{-1}$) | $T_A^*$(K) | Telescope |
|---|---|---|---|---|---|
| CO 2-1 | 10.142 | 7.99 | 5.54 | 1.72 | CSO |
| $C^{18}O$ 2-1 | 0.40 | 7.19 | 0.56 | 1.04 | CSO |
| $HCO^+$ 3-2 | 0.23 | 7.23 | 0.47 | 0.469 | CSO |
| $N_2H^+$ 3-2 | ... | ... | ... | < 0.13 | CSO |
| $N_2D^+$ 3-2 | ... | ... | ... | < 0.30 | CSO |

CB130-3

| | $\int T_A^* dv$(K km s$^{-1}$) | $v_{LSR}$(km s$^{-1}$) | $\Delta v$(km s$^{-1}$) | $T_A^*$(K) | Telescope |
|---|---|---|---|---|---|
| CO 2-1 | 7.77 | 7.59 | 4.51 | 1.62 | CSO |
| $C^{18}O$ 2-1 | 0.55 | 7.16 | 0.49 | 1.28 | CSO |
| $H^{13}CO^+$ 3-2 | 0.36 | 7.18 | 0.48 | 0.70 | CSO |
| $N_2H^+$ | ... | ... | ... | < 0.13 | CSO |
| $N_2D^+$ 3-2 | ... | ... | ... | < 0.15 | CSO |

## Radiative Transfer Modeling

### Radial Intensity Profile

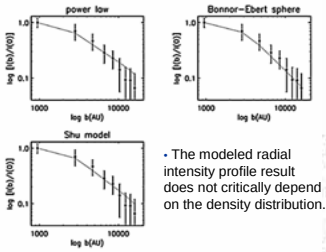


- The modeled radial intensity profile result does not critically depend on the density distribution.

Power law density distribution
n(r) ∝ $r^{-1.8}$ (Shirley et al., 2002)

Disk Temperature distribution
T(r) ∝ $r^{-0.4}$ (flared disk)
→ good for heat absorbing from the central star.

ISRF attenuation
Outside the envelope : $A_V$=2 (CO line fitting)
Inside the envelope: dust opacity model (Pontoppidan, in preparation)

$r_{out}$ = 35000AU comes from its optical size.

### Radiative Transfer Modeling, DUSTY

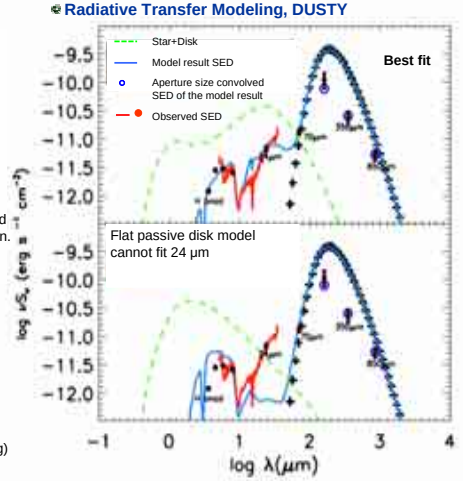


Best fit free parameters
$T_{star}$ = 3000K , $r_{int}$ = 350AU
$L_{star} = 0.03\ L_\odot$, $L_{disk} = 0.12\ L_\odot$

**$L_{int}$ = 0.15 $L_\odot$** > 0.1 $L_\odot$

Not a VeLLO. But still a low luminosity source.

## Line Modeling

### Gas temperature calculation

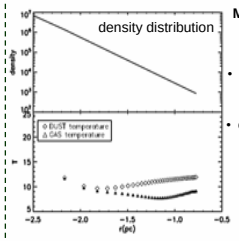


**Model parameters :**

① **The energy transfer between gas and dust**
- The grain cross section per baryon : $6.09 \times 10^{-22} cm^2$

② **The heating by cosmic rays**
- cosmic ray ionization rate : $3.0 \times 10^{-17}\ s^{-1}$

③ **The photoelectric heating**
- The strength of ISRF
  $G(r) = e^{-\tau_{UV}} G_0 = 2.7 \times 10^{-2}\ G_0$
  $A_V = 2$
- $n_e = 0.001 cm^{-3}$

④ **The molecular cooling**
- CO abundance : $7.4 \times 10^{-5}$
- Doppler b parameter : 0.9 km/s

### Abundance : Step function

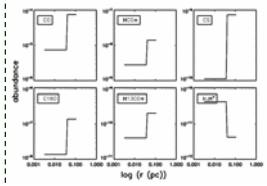


- Center : T < 20K
  → molecule freeze out.
- Outer part : density too low for freeze out
- CO is main destroyer of $N_2H^+$. $N_2H^+$ has reverse abundance profile.

### Monte Carlo Simulation of line profile

Calculate level population of the molecules.

Density distribution, systematic velocity, kinetic temperature, microturbulence and abundance can be considered at the same time, self consistently.

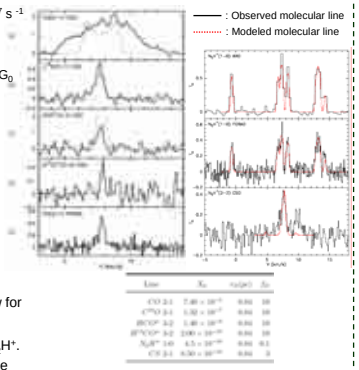


The summary of simulated abundance

## Reference


- Bourke et al., 2006, ApJ, 649, L37 • Clemens & Barvanis, 1988, ApJs, 68, 257 • Dunham et al., 2006, ApJ, 651, 945
- Evans et al., 2003, PASP, 115, 965 • Evans et al., 2005, ApJ,626,919 • Lee & Myers, 1999, ApJs, 123, 233
- Wu et al., 2007, AJ, 133 1560 • Young et al., 2004, 154, 396,